Acta Neuropathol (2004) 107 : 539–545
DOI 10.1007/s00401-004-0848-9

REGULAR PAPER

**J. Patrick van der Voorn · Wout Kamphorst
Marjo S. van der Knaap · James M. Powers**

The leukoencephalopathy of infantile GM1 gangliosidosis: oligodendrocytic loss and axonal dysfunction

Received: 4 August 2003 / Revised: 16 February 2004 / Accepted: 16 February 2004 / Published online: 20 March 2004

Abstract A myelin deficit in the cerebral white matter in infantile GM1 gangliosidosis is well established. Some have proposed this deficit to be secondary to axonal loss, while others argue for delayed or arrested myelination. We compared the frontal white and gray matter of two infants with GM1 gangliosidosis with four age-matched controls, using light microscopy with a quantitative analysis, immunohistochemistry, terminal deoxynucleotidyl transferase-mediated nick-end labeling (TUNEL), and electron microscopy (EM). In the GM1 cases, we found a marked decrease in the number of oligodendrocytes (85% in case 1 and 50% in case 2) and myelin sheaths (80% and 40%), with a mild decrease in axons (20% and 10%). Ultrastructurally, some naked axons and dilated cisterns of rough endoplasmic reticulum (RER) in oligodendrocytes were observed. There was no appreciable storage in remaining oligodendrocytes, nor obvious neocortical neuronal loss. An immunohistochemical decrease in proteolipid protein (PLP) and a more profound deficiency of myelin basic protein (MBP) indicate that this lesion is not simply the result of a delay or arrest in myelination and suggests a "dying-back" oligopathy. TUNEL-positive oligodendrocytes correlated with activated caspase-3 immunoreactivity. Amyloid precursor protein (APP)-immunoreactive aggregates were observed in proximal axons and meganeurites as well as in white matter axons. These data suggest that the myelin deficit results from a loss of oligodendrocytes and abnormal axoplasmic transport, perhaps consequent to massive neuronal storage of GM1.

Keywords Leukoencephalopathy · GM1 gangliosidosis · Apoptosis · Axonal transport

J. P. van der Voorn (✉) · W. Kamphorst
Department of Pathology, Vrije Universiteit Medical Center,
DeBoelelaan 1117, 1007 MB Amsterdam, The Netherlands
Tel.: +31-20-4444008, Fax: +31-20-4442964,
e-mail: jp.vandervoorn@vumc.nl

M. S. van der Knaap
Department of Child Neurology,
Vrije Universiteit Medical Center, Amsterdam, The Netherlands

J. M. Powers
Departments of Pathology and Neurology,
University of Rochester School of Medicine and Dentistry,
Rochester, NY, USA

Introduction

GM1 gangliosidosis is a rare autosomal recessive lysosomal storage disorder caused by a deficiency of lysosomal β-galactosidase, resulting in progressive neural and visceral accumulations of GM1 ganglioside, its asialo derivative GA1, and other minor glycolipids and glycopeptides. Three clinical phenotypes can be distinguished, classified by age of onset: infantile, late infantile/juvenile, and adult. The age of onset and rate of progression of the disease depend on the residual activity of β-galactosidase. Infantile GM1 gangliosidosis, the most common and severe form, is characterized by facial and skeletal abnormalities and neurological deterioration before the age of 6 months. Death usually occurs before the second birthday [24, 25]. Significant white matter abnormalities are present only in the infantile form of GM1 gangliosidosis, but they are also observed in other infantile-onset neuronal storage disorders, such as GM2-gangliosidosis and infantile neuronal ceroid lipofuscinosis (INCL) [1, 25, 26]. A paucity of myelin in GM1 was suggested by several classical neuropathologic and neuroimaging studies of patients and animal models. Neuropathologic examinations have shown decreased myelin staining with minimal axonal degeneration, gliosis, and macrophage infiltration [6, 9]. The typical MRI in GM1 gangliosidosis shows persistent high signal intensity of the white matter on T2-weighted images on serial MR studies, indicating severely defective myelination [12, 20, 25].

Currently we do not understand if and how neuronal storage might lead to white matter pathology. Some possible explanations have been proposed: death of neocortical neurons with axonal loss and secondary loss of myelin, an early arrest of or delay in myelination, primary storage of

ganglioside in oligodendrocytes, a primary oligodendrocytic derangement, or a dysregulation of neuronal-oligodendroglial interactions [5]. Few data to test these hypotheses have been reported. The present investigation aimed to confirm or disprove some of the proposed hypotheses by examining cerebral white and gray matter from two cases of infantile GM1 gangliosidosis, using standard light microscopy with a quantitative analysis, immunohistochemistry, terminal deoxynucleotidyl transferase-mediated nick-end labeling (TUNEL), and ultrastructural analyses.

Materials and methods

Brain tissue was collected for analysis via autopsy at both the Vrije Universiteit Medical Center in Amsterdam (case 1) and the University of Rochester Medical Center in the U.S. (case 2 and the four controls).

Case 1 (male, age 13 months at death, postmortem interval [PMI] 5 h) presented at 5 months of age with failure to thrive. Physical examination showed peripheral and facial edema suggestive of a lysosomal storage disorder. He had abnormal facial features, such as frontal bossing, and lumbar scoliosis. Furthermore, he had poor head control and showed poor visual contact. Fundoscopy revealed bilateral cherry-red spots in the retina, and biochemical studies demonstrated markedly reduced leukocyte β-galactosidase activity. Brain MRI T2-weighted images at 7 months showed a diffusely increased signal in cerebral white matter, indicating a myelin deficiency. There was also an increased signal intensity of the thalamus and only a mild degree of atrophy frontally. Further progression of the boy's severe neurological deficits continued, and he died at 13 months.

Case 2 (female, age 17 months at death, PMI 15 h) presented as a floppy infant at age 3 months. The patient progressively deteriorated, with hypotonia, feeding difficulties, frequent respiratory infections, and, eventually, cortical blindness soon after the 1st year. CT scan indicated increased density of the thalamus and cerebellum. After the classical autopsy findings of GM1 gangliosidosis were identified, reduced β-galactosidase activity was documented.

Four normal control cases of the same age range without neurological disorders were examined for comparison. Ages at death ranged from 5–24 months; causes of death were pulmonary hypertension, pulmonary hemorrhage, dehydration, and sudden infant death syndrome; and PMI at autopsy never exceeded 24 h.

Neuropathology, immunohistochemistry and electron microscopy

The brains were fixed for a minimum of 7 days in formalin before they were sectioned, and selected portions were processed further. Paraffin sections were stained routinely with hematoxylin and eosin (H&E), Luxol-fast blue and periodic acid-Schiff (LFB-PAS), and Bodian silver impregnations.

For quantitative analyses, immunohistochemistry, cell death studies, and electron microscopy (EM) examination, frontal gray and white matter of the two infants with GM1 gangliosidosis were compared to the frontal gray and white matter of four age-matched controls. An indirect immunohistochemical technique using the streptavidin-biotin system was carried out using 3-amino-9-ethylcarbazole (AEC) (ScyTek Laboratories, Logan, UT) as chromagen. Primary antibodies to the following epitopes were used: myelin basic protein (MBP) (R&D Systems, Minneapolis, MN) diluted 1:300, proteolipid protein (PLP)/DM-20 (Chemicon, Temecula, CA) diluted 1:500, platelet-derived growth factor receptor α (PDGFRα) (R&D Systems, Minneapolis, MN) diluted 1:500, NG-2 (Chemicon, Temecula, CA) diluted 1:50, carbonic anhydrase II (CA II) (Rockland, Gilbertsville, PA) diluted 1:15,000, glial fibrillary acidic protein (GFAP) (DAKO, Carpinteria, CA) diluted 1:1,000, amyloid precursor protein (APP) (Chemicon, Temecula, CA) diluted 1:30,000, CD68 (DAKO, Carpinteria, CA) diluted 1:200, Ki67 (DAKO, Carpinteria, CA) diluted 1:1,000, and activated caspase-3 (R&D Systems, Minneapolis, MN) diluted 1:1,000.

Cell death was examined by the TUNEL method. The in situ cell death detection kit (Roche, Indianapolis, IN) was employed according to the vendor's instructions. A negative control without TdT and a positive control (involuted thymus) were treated simultaneously.

For EM, frontal white matter of case 1 was fixed in 2% (v/v) glutaraldehyde and embedded in Epon 812. Ultra-thin sections were collected on 300-mesh Formvar-coated nickel grids. The sections were stained with uranyl acetate and lead citrate and examined in a JEOL 1200 EX electron microscope.

Quantitative morphometry

Numbers of oligodendrocytes – recognized as small cells with uniform round dense nuclei and a perinuclear halo (as confirmed by CA II immunolabeling) – per square unit of tissue were determined on serial sections of frontal white matter in at least 10 standardized microscopic fields of 0.1 mm^2 each, defined by an ocular grid. Relative axonal density was determined in sections stained with Bodian silver impregnations by point sampling, using a 25-point Zeiss eyepiece, as described by Mews et al. [15]: Random points of a grid were superimposed on the sections, and the number of points crossing axons was measured as a fraction of the total number of points of the grid. Axonal density was expressed as the percentage of reduction compared with the normal-appearing white matter (NAWM) of controls. Myelinated fiber density was determined in the same manner with MBP-stained sections.

Results

The fresh brains of cases 1 and 2 weighed 1200 g and 990 g, respectively. Gross examination of both fixed GM1 brains revealed symmetrical atrophic cerebral hemispheres and normal gyral configuration. Moderate dilatation of the ventricles, poor delineation of gray and white matter, firm central white matter, and gray-white discoloration of ganglionic masses were noted on multiple coronal sections. Examination of cerebellum showed atrophic folia, firm white matter, and normal deep nuclei. Sections of midbrain, pons, and medulla showed no abnormalities; sections of spinal cord showed whitish discoloration of the posterior columns at multiple levels.

Microscopically, ballooning of neurons with weakly PAS- and strongly LFB-positive material was noted throughout the central nervous system (CNS). In addition to diffuse neuronal storage, the thalamus and basal ganglia revealed marked gliosis with numerous GFAP-positive reactive astrocytes. Mild astrogliosis was observed throughout the central white matter, with a few CD68-positive macrophages. LFB-stained sections of all white matter regions demonstrated a diffuse paucity of myelin, which was greater in case 1 (Fig. 1A–C). For consistency, frontal lobe was selected for our quantitative, cell death, and EM studies of white matter pathology in infantile GM1 gangliosidosis.

A profound decrease in the number of myelin sheaths was found in the frontal white matter of both cases: a reduction of myelin density of 80% in case 1 and 40% in case 2, when compared with normal white matter. A decrease in immunohistochemically detectable PLP was

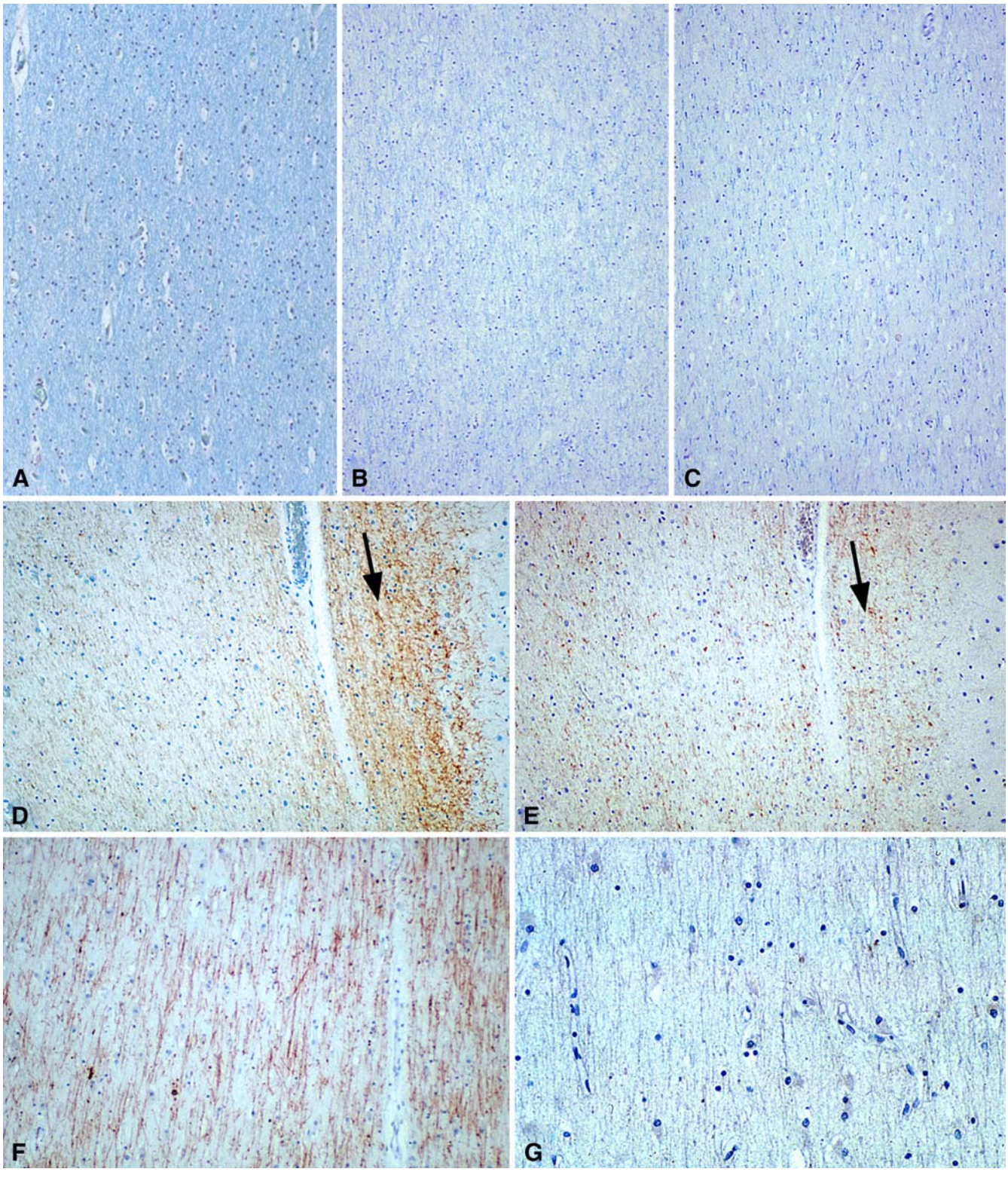

Fig. 1A–G Myelin stainings of cerebral white matter. In contrast to dense myelin staining with LFB seen in controls (**A**), there is a marked depletion of myelinated axons in case 2 (**B**) and even greater in case 1 (**C**). A decrease in immunohistochemically detectable PLP is noted in the arcuate fibers of case 2 (*right side of* **D**, *arrow*) and case 1 (**F**), but the decrease in MBP is greater in case 2 (*right side of* **E**, *arrow*), and, even at higher magnification, virtually no myelin sheaths are labeled in case 1 (**G**). Original magnifications: **A–F** ×37.5; **G** ×75

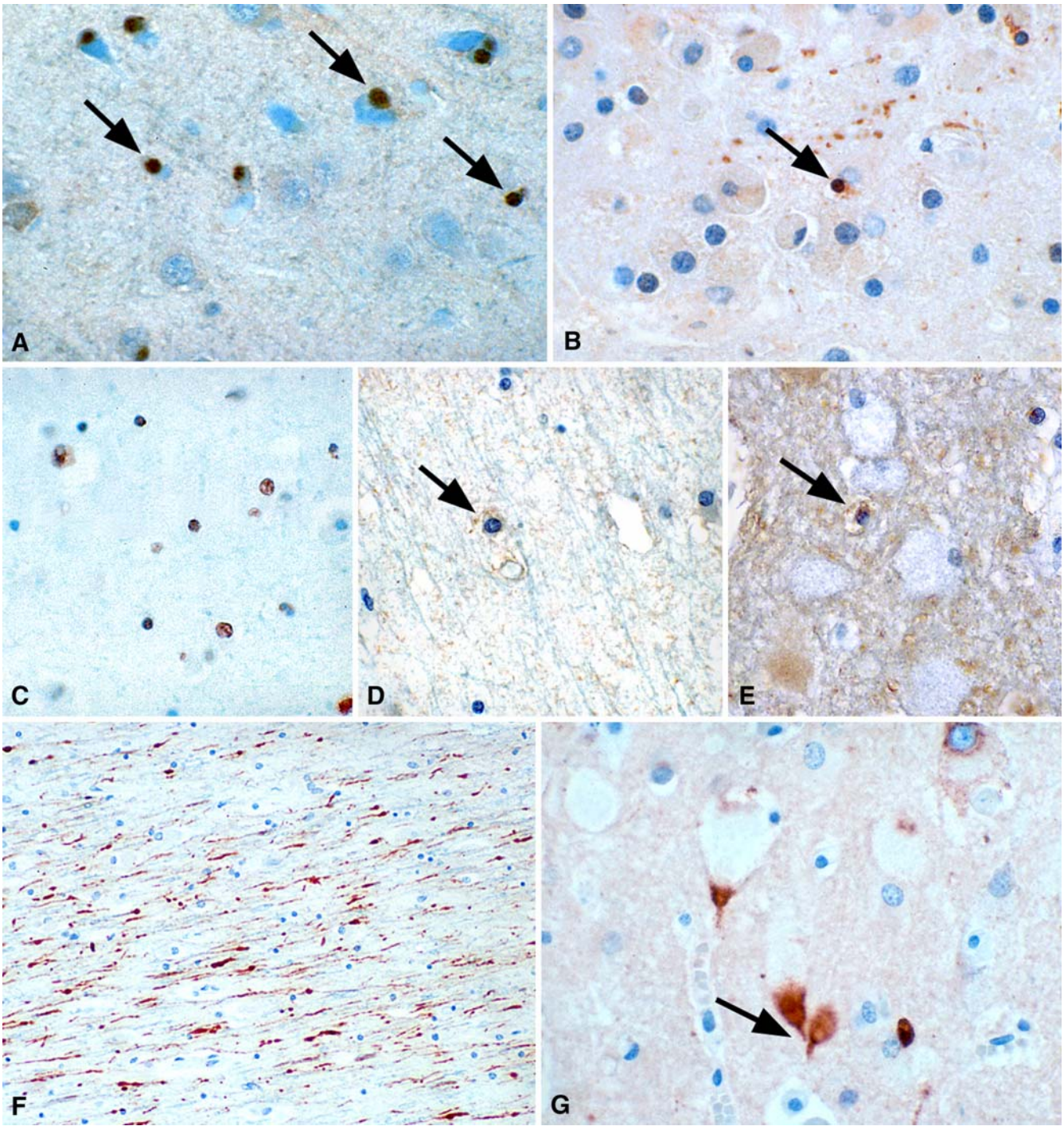

Fig. 2A–G TUNEL and immunohistochemistry for CA II, activated caspase-3 and APP in cerebral white and gray matter. As compared with controls (**A**), decreased numbers of CA II-immunoreactive neocortical oligodendrocytic satellite cells (*arrows*) are observed in case 2 (**B**). Several TUNEL-positive oligodendroglial nuclei are seen in cerebral white matter of case 1 (**C**). Activated caspase-3 positive oligodendrocytes (*arrow*) are observed in cerebral white matter (**D**) and neocortex adjacent to lipidotic neurons (**E**) in case 1. Aggregations of strong APP immunoreactivity are multifocally seen in white matter axons of case 1 (**F**), and increased APP immunoreactivity is observed in neuronal perikarya, their proximal axons, and meganeurites (*arrow*) in case 2 (**G**). Original magnifications: **A, B, D, E, G** ×150, **C** ×100, **F** ×75

noted, but the decrease in MBP in both cases was greater (Fig. 1D–G). In the controls, MBP-immunostaining was always greater than PLP-immunostaining.

Oligodendrocyte numbers in the frontal white matter were reduced relative to control white matter, and comparable decreases in neocortical satellite cells were observed. The remaining oligodendrocytes did not show immunoreactivity for PDGFRα and NG-2, but most oligodendrocytes stained positively for CA II (Fig. 2A–B). On quantification, the average number of oligodendrocytes in the NAWM in controls was 1,100 cells/mm^2. The density

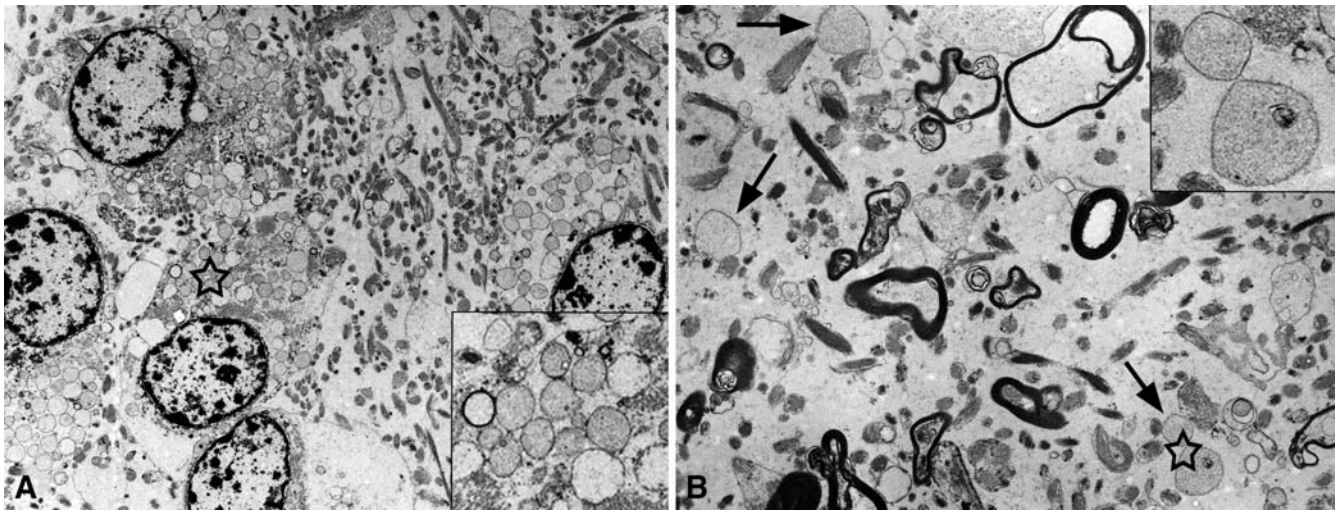

Fig. 3A–B Ultrastructure of case 1 demonstrating swollen mitochondria (artifactual) and dilated cisterns of RER in oligodendrocytes (some of which still display attached ribosomes), containing electron-opaque intraluminal material (**A**) and several naked axons (*arrows*) (**B**) in cerebral white matter. Insets show higher magnification of the areas marked by a star. Original magnifications: **A** ×6,000, **B** ×9,000; inset **A** ×18,000, inset **B**×22,500

of oligodendrocytes in case 1 was 170 cells/mm^2 (85% reduction) and 540/mm^2 in case 2 (50% reduction).

Many oligodendrocytes were TUNEL-positive in both GM1 cases, but astrocytes (Fig. 2C) and, to a lesser degree, the glia of the white matter in some of the control subjects also showed TUNEL positivity. Activated caspase-3 immunoreactivity, a more definitive marker of cells undergoing apoptotic cell death, was seen in oligodendrocytes in both GM1 cases, including satellite oligodendrocytes (Fig. 2D–E). From the observation of serial sections, most of the cells that showed caspase-3 immunoreactivity were also TUNEL positive, whereas TUNEL-positive cells in normal white matter were caspase-3 negative.

Axons were relatively preserved on Bodian silver impregnations. An average axonal loss of 20% in case 1 and 10% in case 2 was observed. Axons appeared intact on the Bodian silver impregnations; however, multiple foci of strong APP immunoreactivity were seen in white matter axons in both cases, and APP was also detected in some neuronal perikarya, their proximal axons, and meganeurites (Fig. 2F–G). With this antibody, at this dilution, we observed no APP immunostaining in the neuronal cell bodies and axons of controls.

Ultrastructurally, the frontal white matter displayed dilated cisterns of rough endoplasmic reticulum (RER) in oligodendrocytes and numerous naked axons, without appreciable ganglioside storage in the majority of residual oligodendrocytes (Fig. 3).

Discussion

Our quantitative data demonstrating a profound decrease in oligodendroglial-myelin units without a comparable decrease in axons and without appreciable loss of neocortical neurons disproves conclusively one of the earliest hypotheses proposed: that the myelin deficit in GM1 gangliosidosis is secondary to neuronal/axonal loss.

Our immunohistochemical and cell death data refute another hypothesis, that the myelin deficiency represents arrested or delayed myelination. The major proteins of the myelin sheath are synthesized in a specific order. The human fetal spinal cord begins to myelinate around 16 weeks after conception [27]. Immunoblot analysis of PLP/DM-20 (the proteolipid class consists of two polypeptides generated through alternative splicing) and MBP in spinal cord homogenates reveals prominent immunoreactive bands corresponding to MBP polypeptides beginning at 16 weeks. A band corresponding to DM-20 is seen at 18 weeks in the absence of PLP, and immunoreactive bands corresponding to PLP and DM-20 are clearly present at 21 weeks of development [10]. Therefore, our finding of a greater deficiency in immunoreactive MBP compared with PLP indicates that the myelin deficiency is not simply the result of a delay or arrest in myelination, and suggests some synthetic defect in the oligodendrocytes of infantile GM1 gangliosidosis. In some toxin-induced demyelinative lesions, the earliest changes in oligodendrocytes occur in their most distal processes before degeneration of the cell bodies occurs, which reflects an inability of the cell to maintain the metabolic processes necessary to support the distal end. This oligodendrocytic abnormality has been referred to as a "dying-back" gliopathy [13]. MBP-mRNA is transported into oligodendrocytic processes where MBP is synthesized on polysomes rather than within the RER of the cell body, such as PLP. Thus, our data raise the possibility of a distal, perhaps "dying-back," oligopathy in GM1 gangliosidosis.

However, our results also showed an absolute decrease in the number of oligodendrocytes.

The finding of activated caspase-3 expressing oligodendrocytes in combination with the detection of DNA fragmentation indicates that the oligodendrocytic decrease is due to their apoptotic death. The observation of dilated RER in residual oligodendrocytes, which resembles the distended RER in oligodendrocytes in Pelizaeus-Merz-

bacher disease [7], suggests a trapping of myelin protein with the consequent release of ER stress signals [22]. The cellular response to ER stress (an imbalance between the load of client proteins facing the ER and the organelle's ability to process that load) involves the upregulation of the capacity to process client proteins and the repression of protein synthesis (lowering the load). This reaction is part of the ER unfolded protein response (UPR). Under sustained ER stress, the upstream UPR components activate pro-apoptotic mechanisms (i.e., activation of caspases), causing apoptotic cell death [8, 17].

The oligodendrocytes that were dying at the time of autopsy appeared to be mature small oligodendrocytes, but precursors may also have been affected, particularly in view of the fact that we were unable to identify any precursors with NG-2 or PDGFRα antibodies. The loss of oligodendrocytes, and perhaps their precursors, may be due to a primary defect in the oligodendrocyte or secondary to abnormal neuronal signals, perhaps consequent to massive neuronal storage of GM1. Significant storage could not be identified in residual oligodendrocytes by LFB staining, confirming an earlier study [6], so lipid storage appears to be an unlikely possibility for their dysfunction or death. The fact that satellite oligodendrocytes in the neocortex were also lost indicates that their death is not necessarily linked to the process of myelination and supports the notion that healthy neuronal signals, such as platelet-derived growth factor (PDGF) [16, 18], may be necessary for oligodendrocytic survival and myelination.

It has been suggested that precursors or formed compounds can be transported from the axon to the nascent myelin sheath. An example is N-acetylaspartate (NAA), which appears to undergo axonal transport and eventual incorporation into myelin lipids through the liberation of its acetyl groups [3]. APP is a protein that is normally transported down the axon by anterograde fast axoplasmic transport. Normal levels of axonal APP are not detectable by standard immunohistochemical techniques, and its detection by this method at sites of axonal injury following head injury [2, 21] and some neurological diseases [4, 11, 14, 19, 23] is thought to represent accumulation of APP due to a failure of axoplasmic transport. Immunostaining for APP in our cases showed multifocal axonal aggregates in the white matter, indicating some degree of axonal dysfunction; perhaps more importantly, APP was also detected in neuronal perikarya and particularly in their proximal axons and meganeurites.

Furthermore, APP immunostainings of cerebral white matter in other leukoencephalopathies (e.g., Canavan disease, X-linked adrenoleukodystrophy, and Alexander disease) have not revealed similar aggregates (unpublished data), suggesting a specific axonal dysfunction in the leukoencephalopathy of infantile GM1 gangliosidosis.

These data imply a defect in fast axoplasmic transport and a possible decrease in the transfer of precursors required for myelin formation, or the loss of some neuronal/axonal signal. The fact that other infantile-onset neuronal storage disorders, such as GM2 gangliosidosis and INCL, have similar white matter abnormalities provides further evidence that the myelin deficiency in all these diseases may be caused by a loss of normal neuronal trafficking and signaling.

Acknowledgments The authors thank Frances Vito for skillful technical assistance. This work was supported by the Dutch organization of Scientific Research (NWO, grant 903-42-097) and the Optimix Foundation for Scientific Research.

References

1. Aronson SM, Volk BW (1962) Pathogenesis of white matter changes in Tay-Sachs' disease. In: Aronson SM, Volk BW (eds) Cerebral spingholipidosis. Academic Press, New York, pp 15–28
2. Blumbergs PC, Scott G, Manavis J, Wainwright H, Simpson DA, McLean AJ (1994) Staining of amyloid precursor protein to study axonal damage in mild head injury. Lancet 344:1055–1056
3. Chakraborty G, Mekala P, Yahya D, Wu G, Ledeen RW (2001) Intraneuronal N-acetylaspartate supplies acetyl groups for myelin lipid synthesis: evidence for myelin-associated aspartoacylase. J Neurochem 78:736–745
4. Ferguson B, Matyszak MK, Esiri MM, Perry VH (1997) Axonal damage in acute multiple sclerosis lesions. Brain 120: 393–399
5. Folkerth RD (1999) Abnormalities of developing white matter in lysosomal storage diseases. J Neuropathol Exp Neurol 58: 887–902
6. Folkerth RD, Alroy J, Bhan I, Kaye EM (2000) Infantile Gm1 gangliosidosis: complete morphology and histochemistry of two autopsy cases, with particular reference to delayed central nervous system myelination. Pediatr Dev Pathol 3:73–86
7. Gow A, Southwood CM, Lazzarini RA (1998) Disrupted proteolipid protein trafficking results in oligodendrocyte apoptosis in an animal model of Pelizaeus-Merzbacher disease. J Cell Biol 140:925–934
8. Kaufman RJ (1999) Stress signaling from the lumen of the endoplasmic reticulum: coordination of gene transcriptional and translational controls. Genes Dev 13:1211–1233
9. Kaye EM, Alroy J, Raghavan SS, Schwarting GA, Adelman LS, Runge V, Gelblum D, Thalhammer JG, Zuniga G (1992) Dysmyelinogenesis in animal model of GM1 gangliosidosis. Pediatr Neurol 8:255–261
10. Kronquist KE, Crandall BF, Macklin WB, Campagnoni AT (1987) Expression of myelin proteins in the developing human spinal cord: cloning and sequencing of human proteolipid protein cDNA. J Neurosci Res 18:395–401
11. Kuhlmann T, Lingfeld G, Bitsch A, Schuchardt J, Bruck W (2002) Acute axonal damage in multiple sclerosis is most extensive in early disease stages and decreases over time. Brain 125:2202–2212
12. Lin HC, Tsai FJ, Shen WC, Tsai CH, Peng CT (2000) Infantile form GM1 gangliosidosis with dilated cardiomyopathy: a case report. Acta Paediatr 89:880–883
13. Ludwin SK, Johnson ES (1981) Evidence for a "dying-back" gliopathy in demyelinating disease. Ann Neurol 9:301–305
14. Medana IM, Day NP, Hien TT, Mai NT, Bethell D, Phu NH, Farrar J, Esiri MM, White NJ, Turner GD (2002) Axonal injury in cerebral malaria. Am J Pathol 160:655–666
15. Mews I, Bergmann M, Bunkowski S, Gullota F, Bruck W (1998) Oligodendrocyte and axon pathology in clinically silent multiple sclerosis lesions. Mult Scler 4:55–62
16. Noble M, Murray K, Stroobant P, Waterfield MD, Riddle P (1988) Platelet-derived growth factor promotes division and motility and inhibits premature differentiation of the oligodendrocyte/type-2 astrocyte progenitor cell. Nature 333:560–562

17. Rao RV, Hermel E, Castro-Obregon S, del Rio G, Ellerby LM, Ellerby HM, Bredesen DE (2001) Coupling endoplasmic reticulum stress to the cell death program. Mechanism of caspase activation. J Biol Chem 276:33869–33874
18. Richardson WD, Pringle N, Mosley MJ, Westermark B, Dubois-Dalcq M (1988) A role for platelet-derived growth factor in normal gliogenesis in the central nervous system. Cell 53: 309–319
19. Sasaki S, Iwata M (1999) Immunoreactivity of beta-amyloid precursor protein in amyotrophic lateral sclerosis. Acta Neuropathol (Berl) 97:463–468
20. Shen WC, Tsai FJ, Tsai CH (1998) Myelination arrest demonstrated using magnetic resonance imaging in a child with type I GM1 gangliosidosis. J Formos Med Assoc 97:296–299
21. Sherriff FE, Bridges LR, Sivaloganathan S (1994) Early detection of axonal injury after human head trauma using immunocytochemistry for beta-amyloid precursor protein. Acta Neuropathol (Berl) 87:55–62
22. Southwood CM, Garbern J, Jiang W, Gow A (2002) The unfolded protein response modulates disease severity in Pelizaeus-Merzbacher disease. Neuron 36:585–596
23. Suenaga T, Ohnishi K, Nishimura M, Nakamura S, Akiguchi I, Kimura J (1994) Bundles of amyloid precursor protein-immunoreactive axons in human cerebrovascular white matter lesions. Acta Neuropathol (Berl) 87:450–455
24. Suzuki Y, Sakuraba H, Oshima A (2001) β-Galactosidase deficiency (β-galactosidosis): GM1-gangliosidosis and Morquio B disease. In: Scriver CR, Beaudet AL, Valle D, Sly WS (eds) The metabolic and molecular bases of inherited disease, 8th edn. McGraw-Hill, New York, pp 3775–3809
25. van der Knaap MS, Valk J (1995) GM1 Gangliosidosis. In: van der Knaap MS, Valk J (eds) Magnetic resonance of myelin, myelination, and myelin disorders, 2nd edn. Springer, Berlin Heidelberg New York, pp 76–80
26. Vanhanen SL, Raininko R, Santavuori P, Autti T, Haltia M (1995) MRI evaluation of the brain in infantile neuronal ceroid-lipofuscinosis. Part 1: Postmortem MRI with histopathologic correlation. J Child Neurol 10:438–443
27. Weidenheim KM, Bodhireddy SR, Rashbaum WK, Lyman WD (1996) Temporal and spatial expression of major myelin proteins in the human fetal spinal cord during the second trimester. J Neuropathol Exp Neurol 55: 734–745